

# Finite-amplitude effects on ultrasound beam patterns in attenuating media

Clarence R. Reilly<sup>a)</sup> and Kevin J. Parker

*Department of Electrical Engineering, and Center for Biomedical Ultrasound, University of Rochester, Rochester, New York 14627*

(Received 21 November 1988; accepted for publication 14 August 1989)

Some problems relevant to medical ultrasonics are addressed through experimental measurements of focused, pure-tone beam patterns under quasilinear conditions where significant nonlinearities are manifested. First, measurements in water provide a comparison of the beam patterns of the fundamental and nonlinearly generated harmonics against recent theoretical predictions of others. The radial beamwidths, presence and spacing of sidelobes, axial distances to peak pressures, focal shock parameter, time-domain waveform asymmetry, and post-focal falloff of the fundamental through fifth harmonics are discussed relative to various models under preshock conditions ( $\sigma < 1$ ). Second, the focused sources are placed in a more attenuating fluid to mimic the behavior of these fields in tissue. The changes in beam characteristics are examined relative to measurements at the same intensities in water, and relative to theoretical predictions. The results suggest that, given a known linear (low-intensity) focused beam pattern in water, guidelines can be followed to predict the beam pattern of the fundamental and higher harmonics at higher intensities in water, and then in attenuating media such as tissue.

PACS numbers: 43.25.Jh, 43.80.Sh, 43.30.Qd

## INTRODUCTION

Finite-amplitude effects in medical ultrasonics can be potentially useful as in the case of lithotripsy, or can degrade system performance as in the case of conventional imaging instruments. Since the works of Carstensen and colleagues,<sup>1-3</sup> much attention has been given to nonlinear wave propagation in ultrasonic fields.<sup>4-15</sup> Parallel research has been underway in underwater acoustics, where the influences of finite-amplitude effects have been studied under different conditions.<sup>16-20</sup> At present, a variety of theoretical approaches and predictions can be applied to the case of medical ultrasound imaging, where frequencies typically range from 2–10 MHz, transducer apertures (when piston or annular array sources are used) are a few centimeters in diameter, and focal lengths can range from less than 3 cm to over 15 cm, depending on application. However, experimental verification of theory, especially in more attenuating media, is limited.

This paper presents experimental studies of focused pure-tone beam patterns within a range of parameters germane to medical ultrasound imaging. The fundamental beam patterns and harmonic beam patterns in preshock conditions (shock parameter  $\sigma \leq 1$  at the focus) are compared with theoretical predictions of others. Included are particular features such as the beamwidth of the harmonics, the presence and location of harmonic sidelobes, the on-axis focal peak of each harmonic, the apparent shock parameter  $\sigma$  at the focal point, the asymmetry of the pressure waveform the post-focal falloff of harmonics, and the effects of attenuation on these parameters.

The results of this study provide practical guidelines for extrapolating from a known linear focused beam to the more complicated case of finite-amplitude propagation at higher intensities, and through tissue.

## I. MATERIALS

Three, 1-in.-diam lead zirconate transducers with fundamental frequencies of 0.59, 2.25, and 3.38 MHz were used to produce quasicontinuous wave beams. The 0.59-MHz transducer was driven at its third (1.75 MHz) and fifth (2.95 MHz) harmonics, while the other transducers were driven at their fundamental frequencies. The transducers were simultaneously mounted in a tank, and concave Lucite lenses were placed 2 mm above each transducer to provide focusing. The lenses were designed to have a nominal focal point of 8 cm in water. Attenuation in the lens resulted in some apodization of the piston sources.<sup>21,22</sup>

A calibrated polyvinylidene fluoride (PVDF) needle-type hydrophone (Medicoteknisk Institut, Denmark) was used as a receiver. The hydrophone had a 1-mm active element and was known to have a nearly flat frequency response from 1 to 12 MHz. The hydrophone sensitivity was determined from total power measurements and hydrophone voltages at the sources to be on the order of 0.022 MPa/mV (16kW/cm<sup>2</sup>/V<sup>2</sup>). A fluid medium was sought to test existing theory on the effect of attenuation on finite-amplitude waves. The ideal medium would have a velocity and  $B/A$  close to water, and an attenuation of 0.02–0.05 Np/cm/MHz in the frequency range of 1–10 MHz. A suitable medium was developed using 49.6 mℓ of a 0.25 molar mixture of 50% mono- and 50% dipotassium phosphate; 1.5 mℓ

<sup>a)</sup> Current address: Indianapolis Center for Advanced Research, Inc., Indianapolis, IN 46104.

Karo corn syrup; and 48.9 mℓ isopropyl rubbing alcohol (90% pure). Alcohol was added to the water/phosphate/sugar mixture to reduce the sound speed and attenuation, and to stabilize the medium against bacterial growth. It is known that the water and alcohol undergo a complex interaction. The addition of alcohol to water apparently increases the relative amount of water in the bound versus free state.<sup>23</sup> In general, the  $B/A$  of a water/alcohol mixture increases rapidly for alcohol volume fractions between 10% and 50%, and then starts to level off. The  $B/A$  of predominantly water and T-butanol mixture ranged from 5–11 in Sehgal *et al.*'s study.<sup>23</sup> Other 50% alcohol solutions such as methanol and isopropanol have measured  $B/A$  values higher than that of water.<sup>24</sup> The difference in the nonlinear parameter of our attenuating medium, assuming  $B/A = 6-10$  ( $\beta = 4-6$ ) relative to water ( $\beta = 3.6$ ), has the effect of increasing the effective shock parameter (or harmonic pressure) by a factor of 1.1–1.7 (0.8–4.6 dB) over the same conditions in water.

The frequency-dependent absorption of our attenuating medium was determined by radiation force insertion loss measurements to be  $0.012f^{1.9}$  Np/cm with  $f$  in MHz (Fig. 1). Although the frequency dependence ( $n = 1.9$ ) is higher<sup>22</sup> than that of tissues ( $n = 1.2-1.3$ ), the nearly square-law function of frequency in the attenuating fluid enables comparison against other theoretical results. The velocity of the attenuating medium was determined to be 1501 m/s using the time of flight of an unfocused 10-MHz nominal frequency pulse. The attenuating medium was recovered after each day of use and tested for a change in the acoustic properties (attenuation and velocity) over time. The attenuation and velocity varied by  $\pm 10\%$  and  $+3\%$  (from 1501 m/s up to 1549 m/s), respectively, over the course of a week. The change in attenuation is within the range of uncertainty of the experimental technique.<sup>21</sup>

## II. PROCEDURES

The spatial-average source intensity  $I_0$  through the lens was determined from radiation force measurements using a

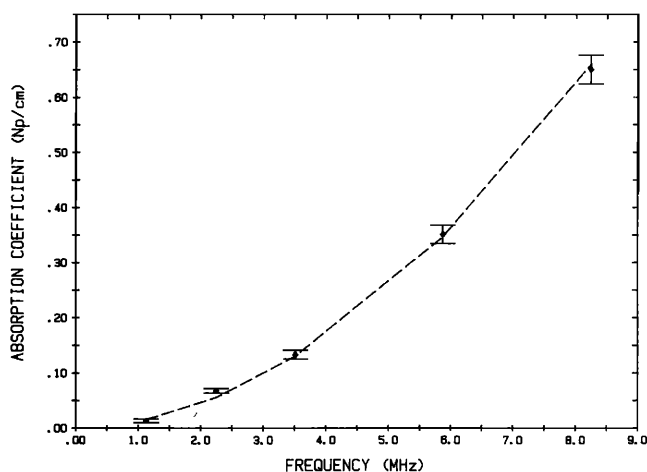


FIG. 1. Frequency-dependent attenuation of water/alcohol/phosphate/sugar mixture. Data points (\*) were fitted to the function  $0.012f^{1.9}$  (---), where  $f$  is in MHz. The standard deviation of the absorption data is shown.

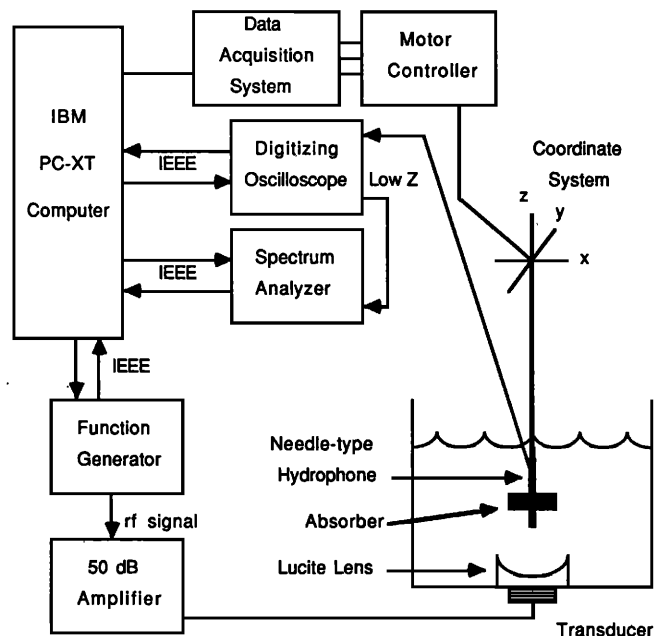


FIG. 2. Automated harmonic data-acquisition system.

rubber absorber and a Sartorius microbalance.<sup>21</sup> Total output power from continuous-wave measurements was divided by source area to determine spatial-averaged intensity and pressure. A linear increase of pressure with voltage was observed, and the results were, in some cases, extrapolated to higher voltages.

Field pressure distributions were determined using the PVDF hydrophone. The 75-W hydrophone cable was connected directly to a Tektronix 7D20 digitizing oscilloscope (40-MHz sampling rate;  $Z_{in} = 1$  MW;  $C_{in} = 20$  pF) as shown in Fig. 2. A low-output impedance amplifier from the oscilloscope was used as a preamplifier for the Tektronix 496P programmable spectrum analyzer. Harmonic beam patterns were obtained through computer control of the signal generator, spectrum analyzer, and stepping motors on a three-axis coordinate system (Velmex Inc., 0.01-mm precision). The Tektronix FG5010 function generator was programmed to send a burst of 100 cycles of a specified frequency every 2 ms. With the spectrum analyzer running asynchronously on maximum hold, the peak values of the first five harmonics at each point within the field (41 points per scan line) were stored in an array after a specified acquisition duration (usually between 8 and 12 s). The point-to-point (incremental) distances for the axial and radial scans at each frequency are given in Table I. The incremental radi-

TABLE I. Incremental scan distances.

Frequency (MHz)	Axial increment (mm)	Lateral increment (mm)
1.75	2.80	0.30
2.25	1.75	0.25
2.94	1.40	0.20
3.38	1.20	0.20

TABLE II. Spatial-average source intensity ( $I_0$ ).

Frequency	Low intensity		High intensity	
	Generator voltage	$I_0$ (W/cm <sup>2</sup> )	Generator voltage	$I_0$ (W/cm <sup>2</sup> )
1.75	0.1	0.049	0.55	1.52
2.25	0.1	0.087	0.5	2.24
2.94	0.2	0.070	0.6	0.92
3.38	0.1	0.071	0.4	1.18

al distance was chosen to include some minor lobes of the beam (only part of a sidelobe is evident at 1.75 MHz) while retaining an adequate resolution.

To observe changes in the harmonic content of the field with intensity, scans at "low"- and "high"- power levels were performed. The power spectrum at low power mainly consisted of linear radiation from the transducer. The high-power level was chosen to approach the upper limit of quasi-

linear shock at the focus for each frequency, while remaining in the linear operating region of the electronic amplifier and sources. Source intensities are given in Table II. The axis of the transducer was determined from lateral scans in orthogonal planes. Axial scans were then performed at the two intensity levels to determine the focal distance for each harmonic. The focal distance was defined as the distance from the center of the lens to the center of the region where the peak amplitude varied by less than  $-0.5$  dB. Lateral beam patterns were obtained at the focus of the fundamental and the second harmonic at the four source frequencies and two intensity levels.

In order to distinguish between linear superposition of transmitted harmonics and nonlinearly generated harmonics in the fluid media, waveforms and spectral content at the acoustic source were measured using the hydrophone. The second harmonic at the source was found to be between  $-25$  and  $-30$  dB below the fundamental at all frequencies and power levels.

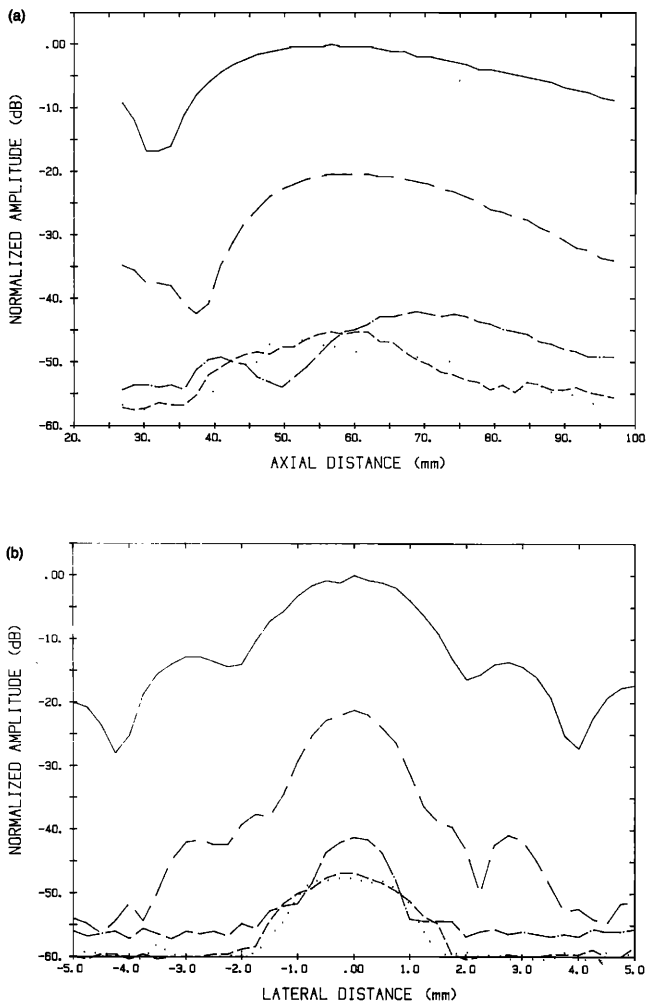


FIG. 3. Axial and lateral beam patterns in water for the 2.25-MHz source at  $I_0 = 0.087$  W/cm<sup>2</sup>. The first (—), second (---), third (— · —), fourth (— · — · —), and fifth (····) harmonics are shown.

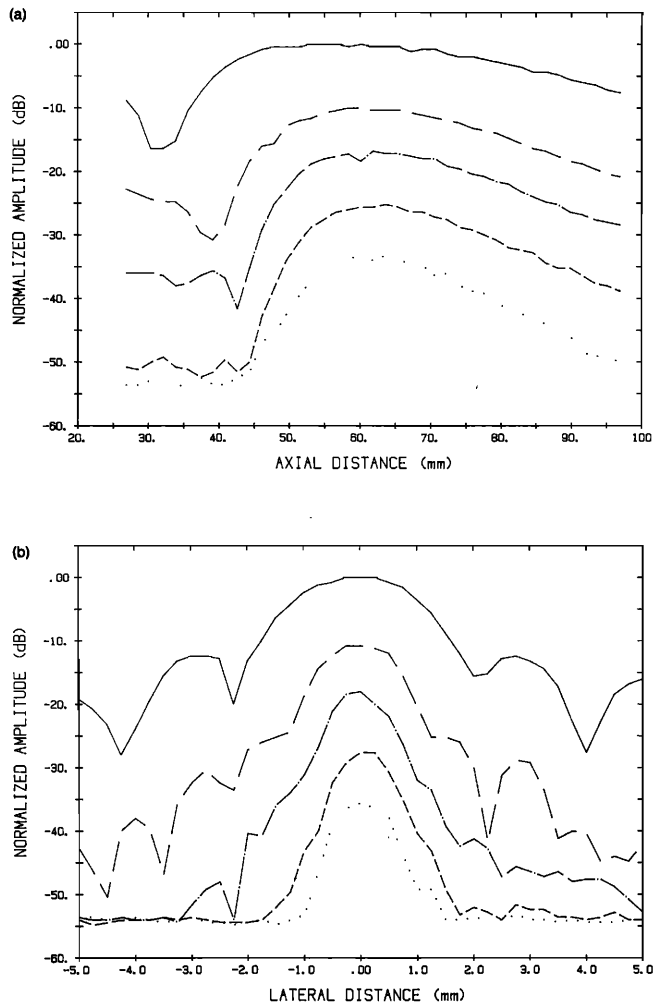


FIG. 4. Axial and lateral beam patterns in water for the 2.25-MHz source at  $I_0 = 2.24$  W/cm<sup>2</sup>. The first (—), second (---), third (— · —), fourth (— · — · —), and fifth (····) harmonics are shown.

### III. RESULTS

The axial and lateral harmonic beam patterns (normalized to the peak fundamental amplitude) in water for the 2.25-MHz low and high intensities are given in Figs. 3 and 4.

In Fig. 3 (low power), the magnitudes of the third through fifth harmonics are barely above the noise floor at approximately  $-55$  to  $-60$  dB. In Fig. 4 (high power), the beam patterns of all harmonics are clearly shown with diffractive sidelobes. Since the hydrophone active element has a 1-mm diameter, fine structures such as the fourth and fifth harmonic sidelobes are not resolved.

High-power beam patterns for all four frequencies are shown in Figs. 5–8, where direct comparisons of the results in water and attenuating fluid are made. The attenuation effects are more significant at higher frequencies and higher harmonics, as expected. Even the highly attenuated beam patterns show strong diffractive effects of sidelobes and axial nulls.

The more traditional examples of time- and frequency-domain representations of one waveform (2.25 MHz), mea-

sured at high intensity at the focus, are given in Fig. 9 for water and Fig. 10 for the attenuating fluid. The higher than expected strength of the sixth through tenth harmonics in Fig. 9(b) is related to the “resonance” of the probe-cable-amplifier circuit which increases gain of frequencies above 12 MHz (Ref. 10).

### IV. DISCUSSION

#### A. Radial beamwidths

As a result of their theoretical derivation, Du and Breazeale<sup>8</sup> predicted that the Gaussian beamwidth for the second harmonic is simply  $1/\sqrt{2}$  times that of the fundamental beamwidth, and a  $1/\sqrt{n}$  relationship for higher harmonic beamwidths was suggested. This is in contrast with  $1/n$  relationship, which would result from the linear propagation of the  $n$ th harmonic from a broadband source.

To test this prediction under our experimental conditions, the  $-6$ -dB harmonic beamwidths in water and the

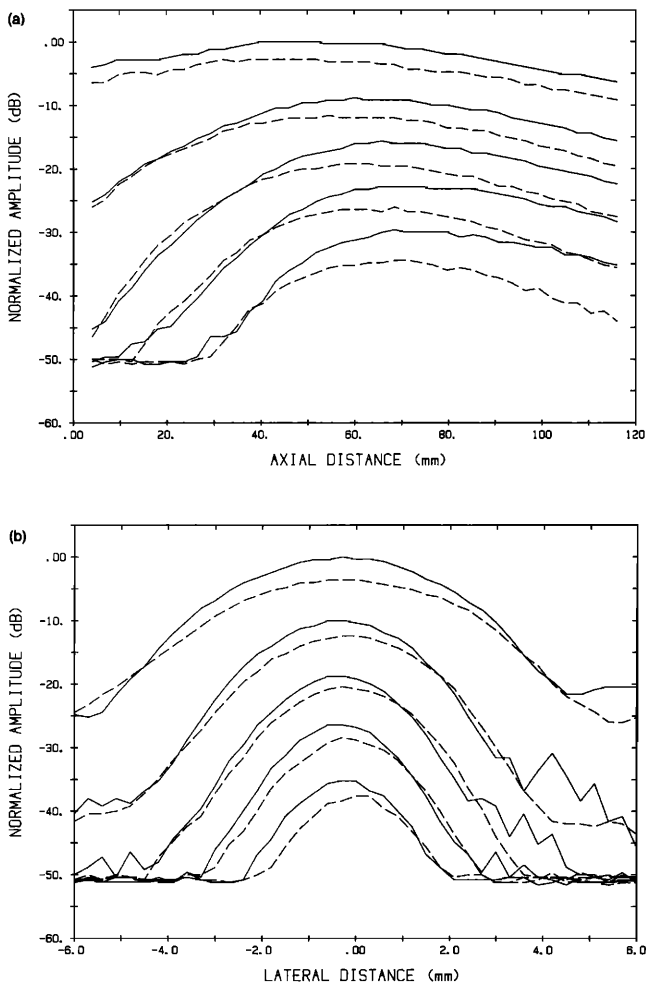


FIG. 5. A comparison of the axial and lateral beam patterns in water and the absorbing fluid for the 1.75-MHz source at  $I_0 = 1.52$  W/cm<sup>2</sup>. The first five harmonics in water (—) and in the absorbing fluid (---) are shown.

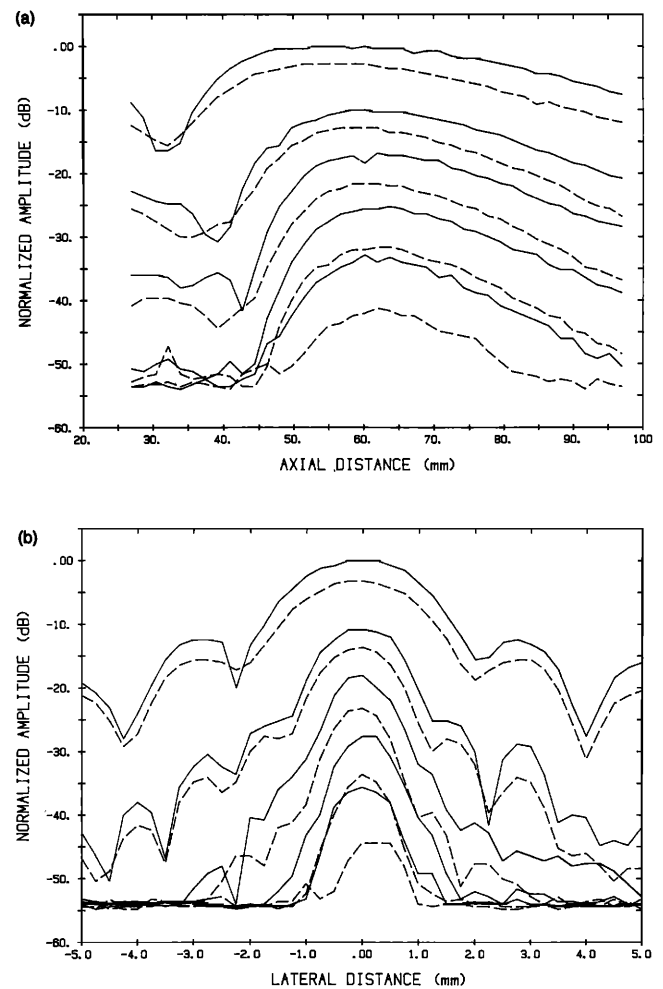


FIG. 6. A comparison of the axial and lateral beam patterns in water and the absorbing fluid for the 2.25-MHz source at  $I_0 = 2.24$  W/cm<sup>2</sup>. The first five harmonics in water (—) and in the absorbing fluid (---) are shown.

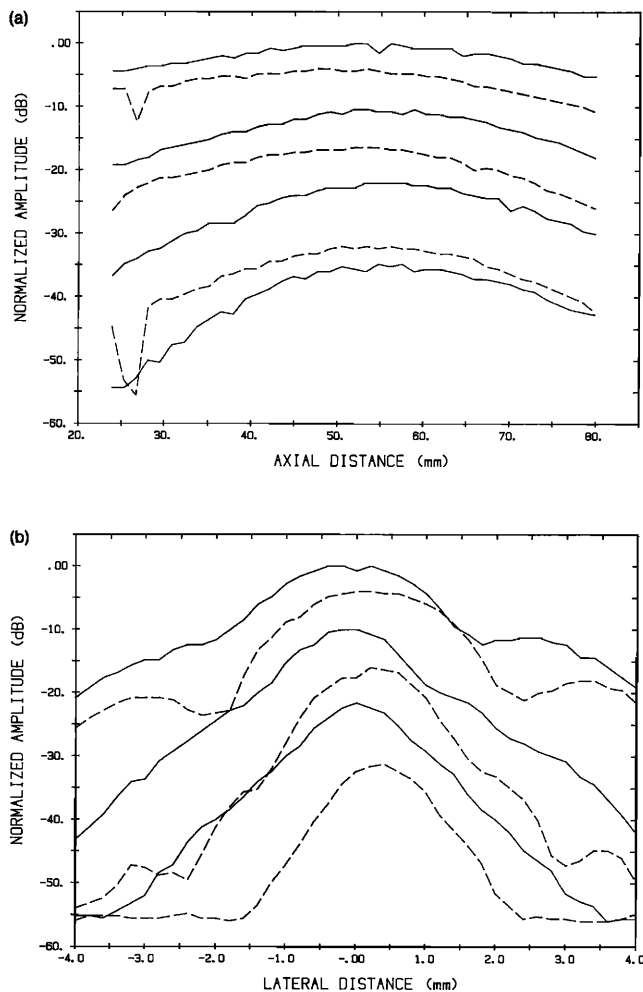


FIG. 7. A comparison of the axial and lateral beam patterns in water and the absorbing fluid for the 2.94-MHz source at  $I_0 = 0.92 \text{ W/cm}^2$ . The harmonics in water (—) and in the absorbing fluid (---) are shown. Four harmonics are shown from the axial beam pattern in water, whereas three harmonics are shown from the beam pattern in absorbing fluid.

attenuating medium at the higher intensities are plotted versus theory for the 1.75- and 3.38-MHz beams in Figs. 11 and 12. The harmonic beamwidth calculations were based on  $1/\sqrt{n}$  times the measured fundamental beamwidth. The theory is generally a good predictor of the non-Gaussian experimental beamwidths at all frequencies.

We note also that only small or insignificant ( $< 0.5 \text{ mm}$ ) changes in measured beamwidths were observed as a function of power, or when comparing results in water versus attenuating fluid.

### B. Harmonic sidelobes

In recent years, some groups have performed numerical solutions to the so-called KZK equation to generate beam patterns of focused piston sources.<sup>17,18,25-27</sup> Their results predict that the second-harmonic beam pattern has twice as many sidelobes as the fundamental component, while the third harmonic has three times as many, and so on. The extra

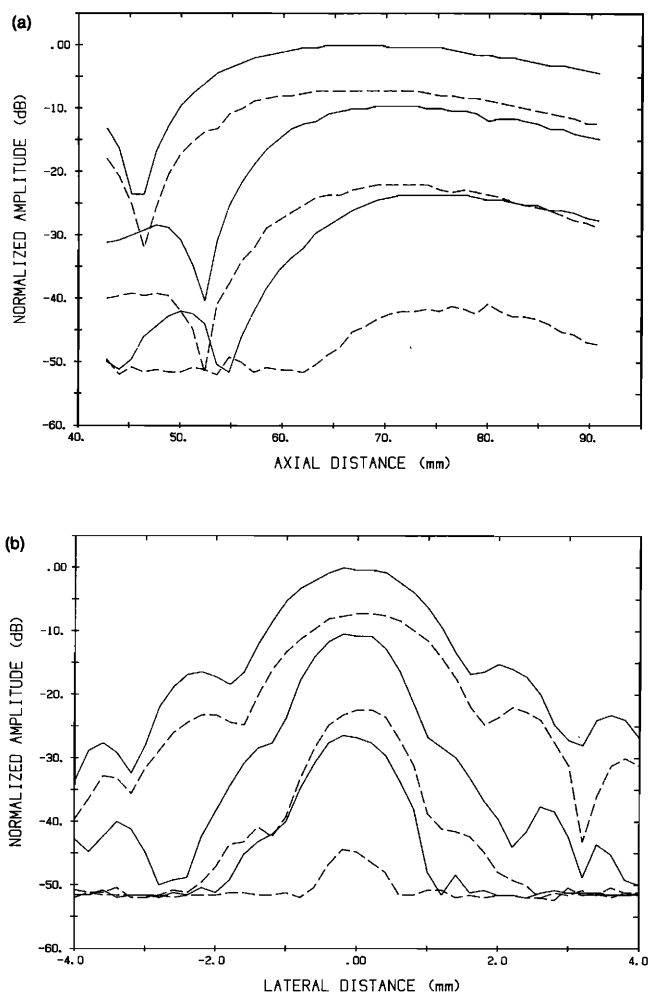
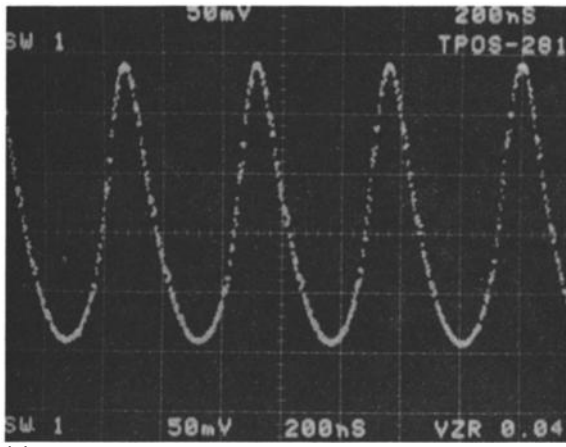


FIG. 8. A comparison of the axial and lateral beam patterns in water and the absorbing fluid for the 3.38-MHz source at  $I_0 = 1.18 \text{ W/cm}^2$ . The first three harmonics in water (—) and in the absorbing fluid (---) are shown.

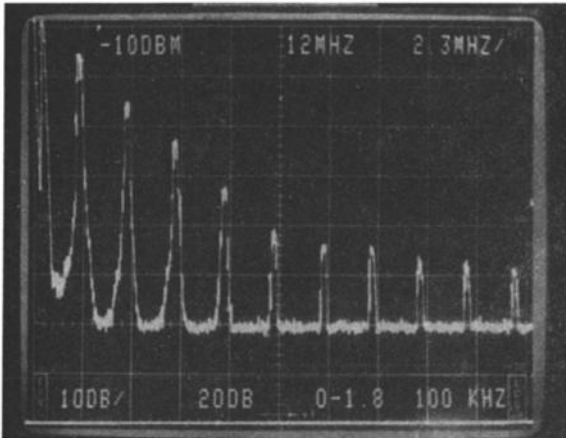
harmonic sidelobes are referred to as “fingers.”<sup>27,33</sup> In our experimental results, the hydrophone 1-mm active element smears much of the fine detail, but the second-harmonic sidelobe doubling can clearly be seen at 2.25 MHz (Fig. 4). At 4.5-mm radial distance, the fundamental beam pattern includes the main lobe and one sidelobe, while the second-harmonic beam pattern includes the main lobe and three sidelobes. Some evidence of this pattern is evident in the third-harmonic pattern. Thus our experimental results agree with the prediction of fingers by Hamilton and colleagues.<sup>17,18,25-27</sup>

### C. Axial peak focal distances

Will the fundamental and second and higher harmonics all reach axial peaks (focal points) at the same distance? The highly focused beams studied by Lucas and Muir,<sup>19</sup> and Hart and Hamilton<sup>26</sup> appear to have coincident axial peaks. However, in the case of Gaussian focused beams studied by Du and Breazeale,<sup>8</sup> the second-harmonic axial peak can be

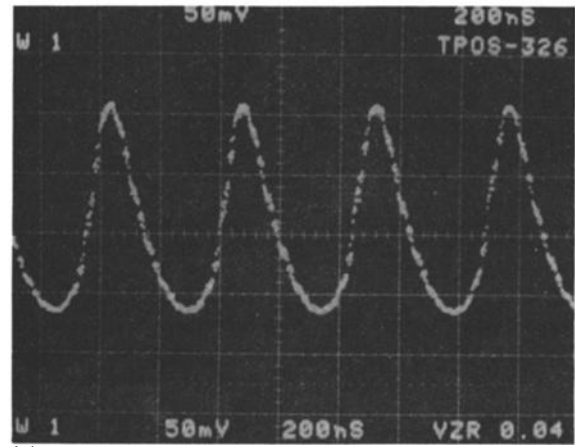


(a)

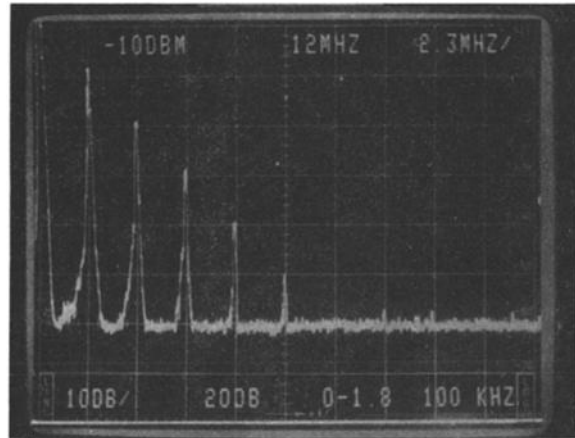


(b)

FIG. 9. The (a) time-domain waveform and (b) its harmonic content at the focus within water for the 2.25-MHz source ( $I_0 = 2.24 \text{ W/cm}^2$ ).



(a)



(b)

FIG. 10. The (a) time-domain waveform and (b) its harmonic content at the focus within the attenuating medium for the 2.25-MHz source ( $I_0 = 2.24 \text{ W/cm}^2$ ).

distal to the fundamental focus, and this is also found to be the case in earlier experimental work of Smith and Beyer<sup>28</sup> and Gould *et al.*<sup>29</sup> In general, our data show that each of the harmonics reach their axial peaks at increasingly distal points compared to the fundamental, as shown in Fig. 13. The influence of attenuation was not strong enough to significantly reverse the trend over the range of frequencies studied. In each case, the geometric focal point is 80 mm from the lens base, while the fundamental axial peaks appeared around 50–70 mm at the four different frequencies studied, as expected from linear theory.<sup>30,31</sup> We note that a linear superposition of harmonics emanating from the source (not generated nonlinearly within the medium) would also exhibit increasing focal lengths with higher frequencies, approaching the geometric focal point of 80 mm in the ideal case of infinitesimal wavelengths. However, in the linear case, as the  $f$  number (focal length to source diameter) is lowered (to produce tighter focusing), the result is closer proximity of axial peaks from different pure-tone excitations. The strong influence of this diffractive effect partially explains the convergence of axial peaks in Lucas and Muir's and Hart and Hamilton's work with low  $f$  number ( $f/2$  tightly focused) beams, as compared to the distal peaks in our experiments (approximately  $f/3$ ) and Du and Brezeale's report on higher  $f$  number (more weakly focused) beams.

#### D. Focal point shock parameter $\sigma$

The shock parameter  $\sigma$  is a useful concept for nondiffracting beams as it describes the relative strength of the harmonic magnitudes and the dependence of  $\sigma$  on position is

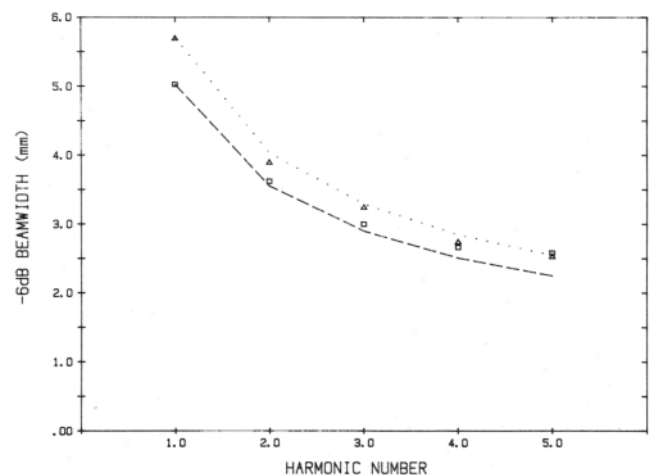


FIG. 11. The  $-6\text{dB}$  harmonic beamwidths for 1.75-MHz source at  $I_0 = 1.52 \text{ W/cm}^2$  compared to  $1/\sqrt{n}$  theory in (a) water: experimental ( $\square$ ), theory (---); and (b) absorbing fluid: experimental ( $\Delta$ ), theory ( $\cdots$ ).

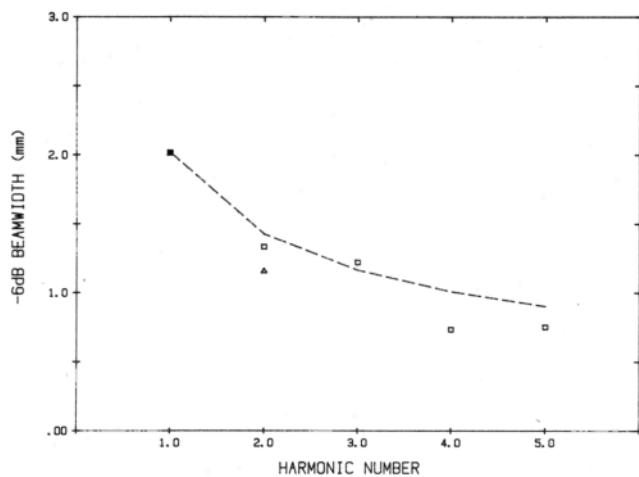


FIG. 12. The  $-6$ -dB harmonic beamwidths for 3.38-MHz source at  $I_0 = 1.18 \text{ W/cm}^2$  compared to  $1/\sqrt{n}$  theory in (a) water: experimental ( $\square$ ), theory (---); and (b) absorbing fluid: experimental ( $\Delta$ ). Since the fundamental beamwidth is the same in the attenuating fluid and in water, the  $1/\sqrt{n}$  theory curves are identical.

a simple, one-dimensional relation for plane and spherical waves.<sup>32,33</sup> In focused beams, the adaptation of a shock parameter is questionable because of the rapidly changing harmonic phases and magnitudes within even the  $-3$ -dB fundamental focal region. Nonetheless, the concept of  $\sigma$  at the fundamental focal point has been employed by others to characterize shock in focused ultrasonic beams. Dalecki<sup>14</sup> applied the relationship for converging spherical waves:

$$\sigma = \beta \epsilon k R \ln(R/r), \quad (1)$$

where  $\epsilon$  is the Mach number (source velocity/speed of sound),  $k$  is the fundamental wavenumber,  $R$  is the effective radius of the spherical source, and  $r$  is the distance back toward the source from the geometric focal point. To avoid the nonphysical, nondiffractive singularity at  $r = 0$ , we applied a simple geometric argument where the minimum  $r$  value was taken to be roughly the axial distance at which the pressure was 0.5 dB below maximum. In comparison, Bacon<sup>4,5</sup> assumed a Gaussian beam shape and derived a different expression for the focal shock parameter:

$$\sigma = \omega \beta P_m F [\ln(G + \sqrt{G^2 - 1}) / \rho c^3 \sqrt{G^2 - 1}], \quad (2)$$

where  $P_m$  is the maximum pressure at the focus,  $G$  is the small signal pressure gain, and  $F$  is the focal distance. Our experimental comparison used measured values of axial beamwidths to estimate  $\sigma$  from Eq. (1), then used pressure

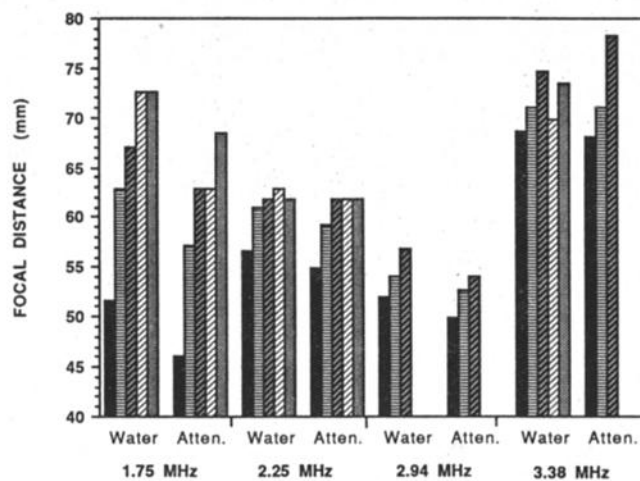


FIG. 13. The location of axial peaks (focal point) for the fundamental and higher harmonics for the four frequencies studied, in water and in the attenuating medium. For each case, shown left to right, are the location of the fundamental (black bar), then the second, third, fourth, and fifth harmonics, respectively. Missing bars indicate insufficient signal above noise.

and gain measurements to estimate  $\sigma$  using Eq. (2). Next, an *ad hoc* estimate of  $\sigma$  was obtained by comparing the harmonic magnitude ratios at the focus to the theoretical description. For example, if the second through fifth harmonics were approximately  $-8$ ,  $-12$ ,  $-15$ , and  $-19$  dB down from the fundamental, this would be labeled as  $\sigma = 1$  since it matches the theoretical<sup>1,32</sup> harmonic ratio for  $\sigma = 1$ . (In the preshock regime,  $\sigma < 1$ , the harmonics are a monotonically increasing function of  $\sigma$ , so there is no ambiguity.) In cases where all harmonics did not match a single  $\sigma$  theoretical result, an estimate was obtained by comparing each harmonic against the fundamental, evaluating the  $\sigma$  for that ratio, and averaging the results over all harmonics. The results are given in Table III.

The shock parameters from spherical wave theory with a minimum  $r$  are less than those predicted from Gaussian theory. The theoretical estimates of  $\sigma$  at 1.75 MHz are much lower than observed. The estimates of  $\sigma$  from the measured harmonic ratios at 2.25 and 2.94 MHz fall between the theoretical values. Both spherical wave and Gaussian theories seem to overestimate experimental values of  $\sigma$  at 3.38 MHz.

In summary, only a rough agreement is found between published techniques for estimating  $\sigma$  at the focus and our measured experimental harmonic magnitudes. This is not surprising since all three techniques use different sets of assumptions, and since the harmonics do not peak coincident-

TABLE III. Theoretical shock parameters for spherically converging and Gaussian sources.

Frequency	$I_0$	$R$ (cm)	$r$ (cm)	$\sigma_{\text{spherical}}$	$p_m$ (MPa)	Gain	$\sigma_{\text{Gaussian}}$	$\sigma_{\text{Harmonic est.}}$
1.75	1.52	5.16	1.4	0.16	0.92	4.22	0.28	0.6
2.25	2.24	5.67	0.9	0.40	2.56	8.11	0.74	0.6
2.94	0.92	5.20	0.56	0.37	2.04	8.45	0.68	0.5
3.38	1.18	6.90	0.78	0.62	2.773	10.45	1.234	0.5

ly with the fundamental, small axial shifts will produce different relative magnitudes and therefore different *ad hoc* estimates of  $\sigma$ .

### E. Asymmetry ratio

Bacon<sup>5</sup> compared experimental and theoretical values of the ratio of peak positive pressure to peak negative pressures,  $P_+/P_-$  of time-domain waveforms in water and an attenuating gel phantom. The conditions (3.5 MHz,  $f/4$  focus) were similar to those in our measurements at 3.38 MHz. Bacon found that in water with the focal shock parameter  $0.2 < \sigma < 1.0$ , the asymmetry ratio ranged between 1.1–1.9. The increased peak positive pressure results from a phase shift between the fundamental and harmonics,<sup>5,10</sup> which is caused by diffraction and dispersion mechanisms. In the attenuating gel, Bacon found the asymmetry ratio reduced to between 1.0–1.05 for the same range of shock parameters. Our measured time domain asymmetry ratios in water and in the attenuating fluid are plotted in Fig. 14 for three source frequencies at high intensities. At 2.25 MHz, there is essentially no change in asymmetry ratio from water to the attenuating fluid. At the two higher frequencies, 2.94 and 3.38 MHz, there are larger differences between asymmetry ratios, as attenuation effects become stronger. Our results at 3.38 MHz are in agreement with those presented by Bacon.

### F. Attenuation loss of harmonics

In linear propagation, the effects of attenuation on a weakly focused beam would be to first approximation:

$$|PA_n(z)| = |PW_n(z)|e^{-\alpha_f n^2 z}, \quad (3)$$

where  $PA_n$  and  $PW_n$  denote  $n$ th harmonic pressure in the attenuating medium and in water, respectively, as a function of axial distance  $z$ . In Eq. (3) a frequency-squared dependence of attenuation is assumed:  $\alpha(n) = \alpha_f n^2$  with  $\alpha_f$  the absorption coefficient at the reference (fundamental) frequency. For plane-wave nonlinear propagation through a

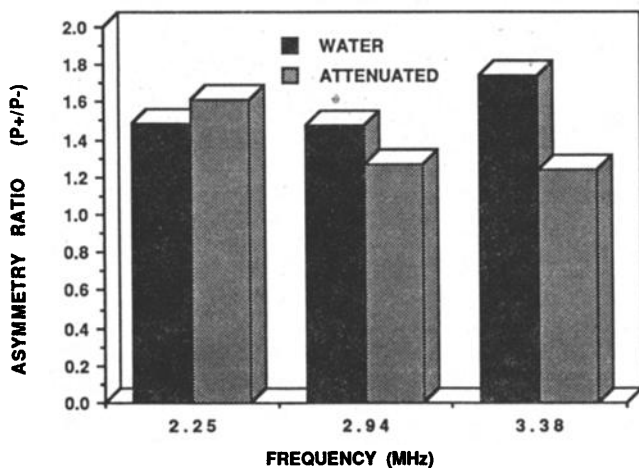


FIG. 14. Asymmetry ratios measured at focal points, in water and in the attenuating fluid, for the three highest frequencies at high intensities.

TABLE IV. Harmonic attenuation at high intensity.

Fre- quency	Measured atten. (dB)			Atten. = $\alpha_f n$ (dB)			$\alpha_0 f^{1.9}$ (dB)		
	1st	2nd	3rd	1st	2nd	3rd	1st	2nd	3rd
1.75	2.8	3.9	3.9	1.5	3.0	4.5	1.5	5.6	12.1
2.25	2.8	4.7	7.1	2.7	5.4	8.1	2.7	10.1	21.8
2.94	4.0	7.9	11.5	4.2	8.4	12.6	4.2	15.6	33.9
3.38	7.2	14.7	20.3	7.1	14.2	21.2	7.1	26.5	57.3

medium of this kind, it has been shown that for  $\sigma \gg 1$ , Fay's solution<sup>34</sup> simplifies to show attenuation of the  $n$ th harmonic as  $e^{-\alpha n z}$ , not as  $e^{-\alpha n^2 z}$ . This is because the fundamental serves as an extended virtual source of the second harmonic, so the decay is not expected to be the same as in linear propagation through a lossy medium. Although the experimental studies presented herein are not plane-wave cases, the attenuation of harmonics generally increased as  $\alpha_f n$ , (linearly with frequency), as opposed to  $\alpha_f n^2$ , (quadratically with frequency) as would be expected from the small signal loss in our attenuating medium. Table IV shows the measured dB difference between the harmonic magnitudes in water and in the attenuating medium as measured at the fundamental focus. (The second- and third-harmonic measured differences have been adjusted for an estimated 2.3-dB difference between the  $\beta$  of the two media.) Also given are predictions of the loss assuming  $\alpha_f n$  and  $\alpha_0 f^{1.9}$  dependences over the distance from the source to the focal point. The linear-with-frequency results are a good match to the data. In soft tissues,<sup>22</sup> where the small signal attenuation coefficients increase as  $f^{1.2}$  or  $f^{1.3}$ , we would still expect the harmonic losses to follow  $n\alpha_f$ , or  $f^{1.0}$ , since the nonlinearly generated harmonics always decay less rapidly than a small signal wave of the same frequency.<sup>35</sup>

Another test of this concept is the decay of harmonics beyond the focal region. The slopes of the harmonics in dB/cm, distal to the focus, were measured in water and in the attenuating fluid. For linear propagation, the expected difference in dB/cm would be equal to the small signal attenuation coefficient at any frequency, which increases as  $f^{1.9}$  or nearly quadratically in our fluid. However, comparisons showed that the axial falloff increased roughly as  $f^{1.0}$ , or linearly with frequency, for the cases studied (Table V). Thus it appears as though quasilinear beam measurements in

TABLE V. Post-focal axial decay (dB/cm): Differences in H<sub>2</sub>O and attenuating fluid at high intensities.

Fre- quency	Measured			Predicted $\alpha = \alpha_f n$			Predicted $\alpha = \alpha_0 f^{1.9}$		
	1st	2nd	3rd	1st	2nd	3rd	1st	2nd	3rd
1.75	0.3	0.4	0.4	0.3	0.6	0.9	0.3	1.1	2.4
2.25	0	1.7	2.3	0.5	1.0	1.5	0.5	1.9	4.0
2.94	0.3	1.1	1.7	0.9	8.4	1.8	0.9	3.3	7.2
3.38	0.8	2.5	3.3	1.1	2.2	3.3	1.1	4.1	8.9

water can be used to predict results in tissues, where the small signal attenuation of the fundamental is applied to the fundamental, twice to the second harmonic, and so forth.

As a final note, Saito *et al.*<sup>20</sup> described the ratio of fundamental to second harmonic as being relatively constant beyond the focal region in their study. However, in all cases reported herein, the second and higher harmonics had increasingly steeper slopes (by 1–3 dB/cm) compared to the fundamental falloff beyond the focus.

## V. CONCLUSIONS

Focused, radially symmetric, ultrasound beams in the low-MHz medical ultrasound band have been studied to determine finite-amplitude effects in water and in an attenuating fluid. Comparisons have been made against theoretical and experimental results of others. Specific results can be summarized as follows.

(1) The  $-6$ -dB beamwidths of the harmonics decrease as  $1/\sqrt{n}$ , where  $n$  is the harmonic number, in accordance with the theoretical results for Gaussian beams obtained by Du and Breazeale.<sup>8</sup>

(2) The sidelobes of the harmonic beam patterns exhibit  $n$  times the number of lobes found in the radial beam pattern of the fundamental, confirming the theoretical prediction of fingers by the Tjottas, Hamilton, and colleagues.<sup>18,25,27</sup>

(3) The axial peaks (or focal points) of harmonics are distal to the fundamental focus, in accordance with the results expected from linear diffraction theory.

(4) Attenuation does not significantly change the  $1/\sqrt{n}$  beamwidth relation or finger patterns. Attenuation causes a small shift in the focal peaks towards the source; however, the harmonics still have axial peaks distal to the fundamental peak.

(5) The ratio of harmonics at the fundamental focus in water can be roughly estimated from  $\sigma$  calculations using spherical converging wave [Eq. (1)] or modified Gaussian [Eq. (2)] approaches.

(6) The asymmetry ratio of the time-domain waveforms at the focus drops from approximately 1.8 in water to 1.2 in the attenuating medium at 3.35 MHz, in general agreement with Bacon's results.

(7) The loss of harmonics in the attenuating medium (compared to water) is proportional to  $\alpha_f n z$ , instead of the nearly  $\alpha_f n^2 z$  frequency dependence of small signals in our lossy fluid. This result is especially significant, since it parallels earlier plane-wave and spherically diverging wave results and provides a simple rule for extrapolating beam patterns measured in water to beam patterns in lossy media such as tissues.

It is possible to use different approaches with numerical methods to calculate beam patterns under a variety of conditions. This experimental work and comparisons provide guidelines for general understanding and prediction of behaviors in the quasilinear regime. Specifically, for a given radially symmetric source, a linear beam pattern can be calculated by conventional means. Then, the magnitude of harmonic, beamwidths, and sidelobe patterns can be esti-

mated using the results of Sec. IV A, B, and D. The location of axial peaks can be crudely estimated using the results of Sec. IV C. Then, the changes produced by propagation in a lossy medium can be estimated using the simple  $a_f n$  results of Sec. IV F. This should be useful in predicting finite-amplitude effects of medical ultrasound equipment in tissues and other related applications.

## ACKNOWLEDGMENTS

The insight, encouragement, and support of Professor E. L. Carstensen and Professor D. T. Blackstock are sincerely appreciated. This work was supported in part by NIH Grant No. CA39241.

<sup>1</sup>T. G. Muir and E. L. Carstensen, "Prediction of nonlinear acoustic effects at biomedical frequencies and intensities," *Ultrasound Med. Biol.* **6**, 345–357 (1980).

<sup>2</sup>E. L. Carstensen, W. K. Law, N. D. McKay, and T. G. Muir, "Demonstration of nonlinear acoustical effects at biomedical frequencies and intensities," *Ultrasound Med. Biol.* **6**, 359–368 (1980).

<sup>3</sup>E. L. Carstensen, N. D. McKay, D. Dalecki, and T. G. Muir, "Absorption of finite amplitude ultrasound in tissues," *Acoustics* **51**(1), 116–123 (1982).

<sup>4</sup>D. R. Bacon, "Finite amplitude distortion of pulsed fields used in diagnostic ultrasound," *Ultrasound Med. Biol.* **10**(2), 189–195 (1986).

<sup>5</sup>D. R. Bacon, "Finite amplitude propagation in acoustic beams," Ph.D. thesis, University of Bath (1986).

<sup>6</sup>G. Du and M. A. Breazeale, "The ultrasonic field of a Gaussian transducer," *J. Acoust. Soc. Am.* **78**, 2083–2087 (1985).

<sup>7</sup>G. Du and M. A. Breazeale, "Harmonic distortion of a finite amplitude Gaussian beam in a fluid," *J. Acoust. Soc. Am.* **80**, 212–216 (1986).

<sup>8</sup>G. Du and M. A. Breazeale, "Theoretical description of a focussed Gaussian ultrasonic beam in a nonlinear medium," *J. Acoust. Soc. Am.* **81**, 51–57 (1987).

<sup>9</sup>K. J. Parker, "Observation of nonlinear acoustic effects in a B-scan imaging instruments," *IEEE Trans. Sonics Ultrason.* **SU-32**(1), 4–8 (1985).

<sup>10</sup>K. J. Parker and E. M. Friets, "On the measurement of shock waves," *IEEE UFFC* **34**(4), 454–460 (1987).

<sup>11</sup>D. Rugar, "Resolution beyond the diffraction limit in the acoustic microscope: A nonlinear effect," *J. Appl. Phys.* **56**(5), 1338–1346 (1984).

<sup>12</sup>H. C. Starritt, M. A. Perkins, F. A. Duck, and V. F. Humphrey, "Evidence for ultrasonic finite amplitude distortion in muscle using medical equipment," *J. Acoust. Soc. Am.* **77**, 302–306 (1985).

<sup>13</sup>W. Swindell, "A theoretical study of nonlinear effects with focussed ultrasound in tissues: An Acoustic Bragg peak," *Ultrasound Med. Biol.* **11**(1), 121–130 (1985).

<sup>14</sup>D. Dalecki, "Nonlinear absorption of focussed ultrasound and its effect on lesion thresholds," MS thesis, University of Rochester (1985).

<sup>15</sup>M. E. Haran and B. D. Cook, "Distortion of finite amplitude ultrasound in lossy media," *J. Acoust. Soc. Am.* **73**, 774–779 (1983).

<sup>16</sup>S. I. Aanonsen, T. Barkve, J. N. Tjøtta, and S. Tjøtta, "Distortion and harmonic generation in the nearfield of a finite amplitude sound beam," *J. Acoust. Soc. Am.* **75**, 749–768 (1984).

<sup>17</sup>M. F. Hamilton, "Fundamentals and applications of nonlinear acoustics," in *Nonlinear Wave Propagation in Mechanics-AMD*, edited by T. W. Wright, ASME Symposium on Nonlinear Wave Propagation (ASME, New York, 1986), Vol. 77.

<sup>18</sup>M. F. Hamilton, J. N. Tjøtta, and N. Tjøtta, "Nonlinear effects in the farfield of a directive sound source," *J. Acoust. Soc. Am.* **78**, 202–216 (1985).

<sup>19</sup>B. G. Lucas and T. G. Muir, "Field of a finite-amplitude focusing source," *J. Acoust. Soc. Am.* **74**, 1522–1528 (1983).

<sup>20</sup>S. Saito, B. C. Kim, and T. G. Muir, "Second harmonic component of a nonlinearly distorted wave in a focussed sound field," *J. Acoust. Soc. Am.* **82**, 621–628 (1987).

- <sup>21</sup>K. J. Parker and M. E. Lyons, "Absorption and attenuation in soft tissues: I-Calibration and error analysis," *IEEE UFFC* **35**(2), 242-252 (1988).
- <sup>22</sup>M. E. Lyon and K. J. Parker, "Absorption and attenuation in soft tissues II-Experimental results," *IEEE UFFC* **35**(4), 511-521 (1988).
- <sup>23</sup>C. M. Sehgal, B. Poter, and J. F. Greenleaf, "Relationship between acoustic nonlinearity and the bound states of water," *IEEE Ultrason. Symp.* 883-886 (1988).
- <sup>24</sup>L. Germain, R. Z. Jacques, and J. Cheeke, "Nonlinear generation of harmonics near the focus of an acoustic lens," *IEEE Ultrasonic Symposium Proceedings* (1988).
- <sup>25</sup>T. S. Hart and M. F. Hamilton, "Nonlinear effects in focussed sound fields," *Proc. 11th Int. Symp. on Nonlinear Acoustics, Novosibirsk, USSR* (1987).
- <sup>26</sup>T. S. Hart and M. F. Hamilton, "Nonlinear effects in focused sound fields," *J. Acoust. Soc. Am.* **84**, 1488-1496.
- <sup>27</sup>J. Berntsen, J. Tjøtta, S. Tjøtta, "Nearfield of a large acoustic transducer, Part IV," *J. Acoust. Soc. Am.* **75**, 1383-1391 (1984).
- <sup>28</sup>C. Smith and R. T. Beyer, "Ultrasonic radiation field of a focusing source at finite amplitudes," *J. Acoust. Soc. Am.* **46**, 806-813 (1969).
- <sup>29</sup>R. K. Gould, C. W. Smith, A. O. Williams, and R. P. Ryan, "Measured structure of harmonics," *J. Acoust. Soc. Am.* **40**, 421-427 (1966).
- <sup>30</sup>G. Kossoff, "Analysis of focusing action of spherically curved transducers," *Ultrasound Med. Biol.* **5**, 359-365 (1979).
- <sup>31</sup>N. Born and E. Wolf, *Principles of Optics* (Pergamon, New York, 1980), 6th ed., p. 435.
- <sup>32</sup>D. T. Blackstock, "Connection between the Fay and Fubini solutions for plane sound waves of finite amplitude," *J. Acoust. Soc. Am.* **39**, 1019-1026 (1966).
- <sup>33</sup>J. C. Lockwood, T. G. Muir, and D. T. Blackstock, "Directive harmonic generation in the radiation field of a circular piston," *J. Acoust. Soc. Am.* **53**, 1148-1153 (1973).
- <sup>34</sup>R. D. Fay, "Plane sound waves of finite amplitude," *J. Acoust. Soc. Am.* **3**, 222-241 (1931).
- <sup>35</sup>D. A. Webster and D. T. Blackstock, "Experimental investigation of outdoor propagation of finite amplitude noise," *NASA Contractor Rep. 2992* (1978).